Proceedings of the XXXVI Zakopane School of Physics, Zakopane 2001

Magnetic Textures in Thin Ion-Irradiated Ni and Fe Films*

K.P. Lieb[a], Kun Zhang[a], G.A. Müller[a], P. Schaaf[a], M. Uhrmacher[a], W. Felsch[b] and M. Münzenberg[b]

[a]II. Physikalisches Institut, Universität Göttingen
Bunsenstr. 9, 37073 Göttingen, Germany
[b]I. Physikalisches Institut, Universität Göttingen
Bunsenstr. 9, 37073 Göttingen, Germany

Heavy-ion bombardment of thin ferromagnetic, polycrystalline films can induce substantial changes of their magnetic and microstructural properties. Since we first identified this effect in 50–150 nm thick Fe and Ni films irradiated with Xe-ions, we made a systematic search for the influence of various film and implantation parameters on the orientation and degree of the magnetic anisotropy and how these parameters correlate with the microstructure of the films. Several analyzing methods, such as Rutherford backscattering, magneto-optical Kerr effect, X-ray diffraction, magnetic force microscopy, ^{111}In perturbed angular correlation, and conversion electron Mössbauer spectroscopy, were employed in the investigation.

PACS numbers: 75.30.Gw, 75.50.Bb, 75.70.Ak

1. Introduction

Micromagnetism, i.e. magnetic properties of thin layers and other nanometer structures, is a challenge in physics and technology, due to its importance in magnetic sensorics and data storage. The high radiation damage density, which energetic ions deposit locally in solids, can have a profound influence on the micro and domain structure in ferromagnetic films. This influence is visible as flux pinning, ion-induced grain growth, accumulation of defects, and magnetostriction [1, 2]. As examples, we mention the patterning of Co/Pt multilayers [3–5] or FePt

*Supported by Deutsche Forschungsgemeinschaft.

chemically-ordered superlattice films [6] by ion irradiation. The Orsay group succeeded in producing dipolar coupled Ising dots in thin Co/Pt multilayers, irradiated with a He beam. The domain walls were only few nm thick and the ion irradiation at 3×10^{16} α-particles/cm^2 was sufficient to reduce the coercive field from 180 Oe to 25 Oe [3–5]. Concerning the particular case of noble-gas ion implantation into elemental ferromagnetic films, to which we refer in the present work, we mention investigations of the Stanford group [7]. They carried out experiments on ion-beam assisted sputter deposition (IBAD) under 100 eV Xe-bombardment at inclined incidence. These experiments resulted in a pronounced magnetic anisotropy within the film plane, which was related to an uniaxial lattice compression within the film plane and a dilatation vertical to it. Inverse magnetostriction was considered the dominating source of the magnetic anisotropy.

2. Early experiments

Magnetic anisotropy of thin Fe films during low-temperature Xe irradiations was found in 1996 by Neubauer, Reinecke et al. [8–10] in their studies of ion beam mixing effects in Ag/Fe bilayers and of the hyperfine interactions in laser-deposited AgFe and InFe alloys. For the thermally non-miscible system Ag/Fe it turned out that the heavy-ion induced collisional interface mixing is counterbalanced by segregation of the intermixed layer during the spike condensation phase [8–10]. The surprising result was that the *interface roughness* did not increase significantly during ion implantation. This was also confirmed by Kurowski via X-ray diffraction in Ag/Fe multilayers [11]. Proof of the magnetic texturing effect in this system occurred via perturbed angular correlation (PAC) spectroscopy with ^{111}In tracers, which were either ion-implanted or deposited as a submonolayer in Fe, at a distance of few nm from the interface [12]. As can be seen in Fig. 1, the PAC spectra and their Fourier transforms show a pronounced magnetic texturing effect [8]. These data clearly exhibit a dramatic change of the magnetization pattern during the Xe-irradiation: the component having the Larmor frequency ω_L is strongly reduced in intensity relative to the component having $2\omega_L$. By means of the Mössbauer spectroscopy we showed that the hyperfine field is oriented within the film plane after irradiation, while it was more or less isotropic after deposition (see below).

A similar texturing effect was also found [13] when measuring the magnetization curves of Ag/Fe bilayers or Fe films via magneto-optical Kerr effect (MOKE). We noted that the coercive field strength H_c strongly decreased during irradiation and reached values about twice those obtained for 15 nm thick single-crystalline Fe films and magnetized along the $\langle 110 \rangle$ hard or $\langle 100 \rangle$ easy direction [14]. PAC and MOKE analyses were also carried out for 18–400 nm thin Ni films deposited on Si or SiO_2 substrates and irradiated at 100–300 K with Xe^+ beams [15]. In order to ensure that no ion-beam induced nickel silicide formation occurred at the Ni/Si interface [16], the ion energy was chosen such that the mean ion range was less

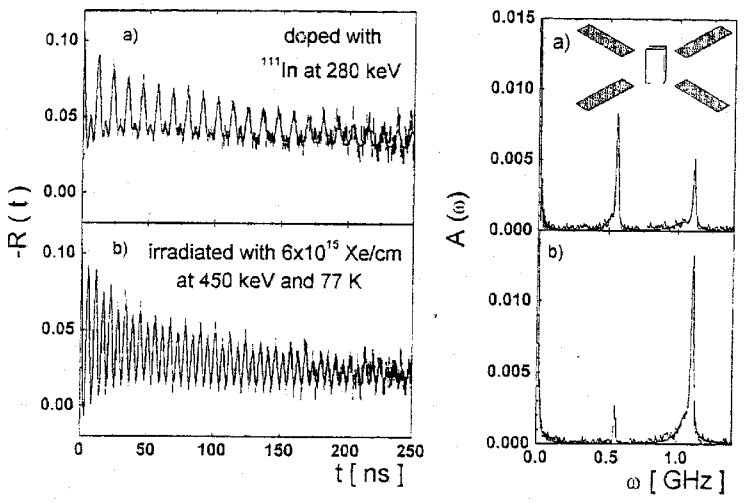

Fig. 1. PAC spectra of a Ag/Fe bilayer doped with ^{111}In ions taken before (a) and after (b) an irradiation with 450 keV Xe ions at 100 K. Note the strong changes of the ω_L and $2\omega_L$ components in the spectra [8].

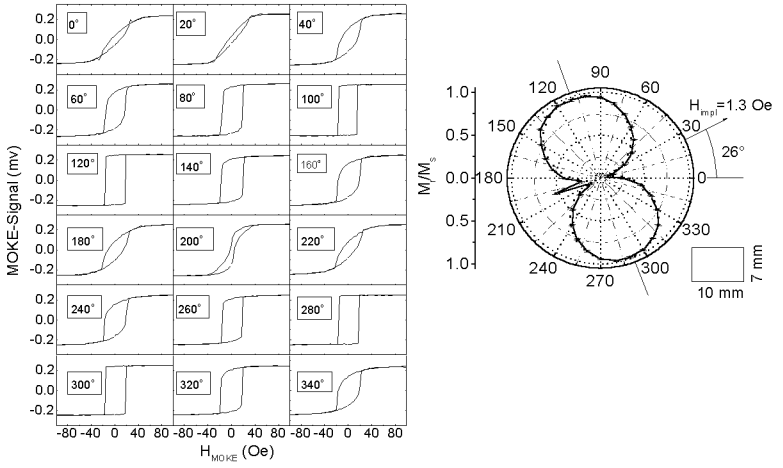

Fig. 2. Magnetic anisotropy of a 75 nm thick polycrystalline Ni-film on Si ⟨100⟩ irradiated at 100 K with 4×10^{14} Xe-ions/cm^2 at 200 keV. The right-hand part is a polar diagram of the relative remanence.

than half the Ni thickness. Figure 2 illustrates the magnetization curves measured at various angles θ between the external magnetic field H and the orientation of the sample as indicated for example by the direction of the long axis. Like in the case of Fe, one notes that an ion fluence as small as 4×10^{14} Xe ions/cm^2 drastically reduces the coercive field to 20–30 Oe. Further irradiations did have much

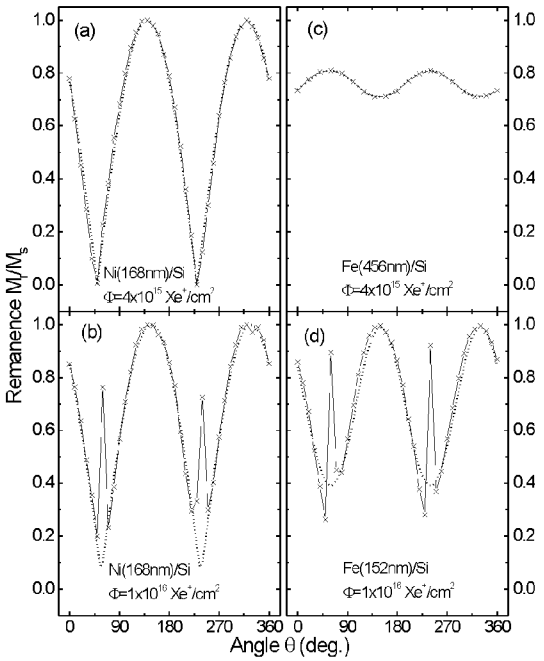

Fig. 3. Comparison of the relative magnetic remanence in Ni and Fe films of various thicknesses generated by Xe-irradiations at 100 K and with fluences of 4×10^{15} and 1×10^{16} ions/cm^2.

influence on the magnetization pattern. The hysteresis depends strongly on the angle θ (compare the data taken at $\theta = 0°$, $90°$ and $\theta = 40°$!).

In Fig. 3, the angular dependences of the relative remanence $\mathcal{R}(\theta) = M_\mathrm{r}/M_\mathrm{s}$ for Fe and Ni films irradiated with 4×10^{15} or 1×10^{16} Xe ions at 100 K are compared. One notes similar effects in both matrices at similar film thicknesses, but a much smaller texturing in the case where the film thickness is much larger than the ion range calculated via TRIM [17].

3. Magnetic texturing in Ni films: the influence of external strain and magnetic fields during ion irradiation

Our previous PAC and MOKE analyses of ion-irradiated Ni films [15, 18] did not take particular care concerning the various types of stresses in the samples. However, inverse magnetostriction as one of the basic mechanisms generating magnetic anisotropies depends on these stresses [1, 2]. There are usually strains either induced during deposition of the films or produced by the implanted ions and possibly by external stresses, due to the mounting or cooling of the samples. In order to disentangle their relative influence, we carried out two types of experiments for 75 nm Ni films irradiated with 250 keV Xe-ions at 100 K.

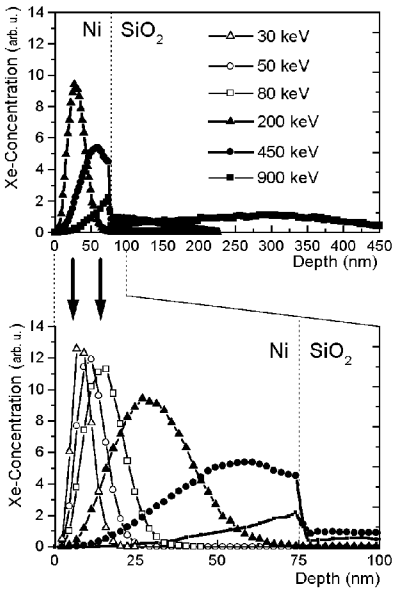

Fig. 4. Implantation profiles of 30–900 keV Xe-ions in a Ni(75 nm)/SiO_2 bilayer.

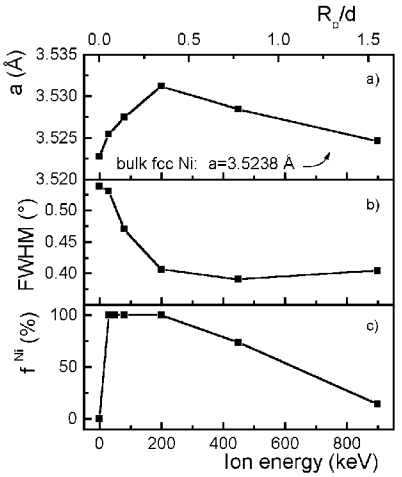

Fig. 5. (a) Lattice constant a, (b) FWHM of (111) reflex, and (c) fraction f^{Ni} of Xe-ions stored in the Ni layer, versus ion energy.

In the first series, the ion energy was varied between 30 and 900 keV, i.e. in such a manner that the projected ion range R_{p} was located either near the surface, in the center of the Ni film, at the layer/backing interface, or finally in the SiO_2 substrate. The calculated Xe distributions are illustrated in Fig. 4. We analyzed these films at room temperature before and after the Xe implantations,

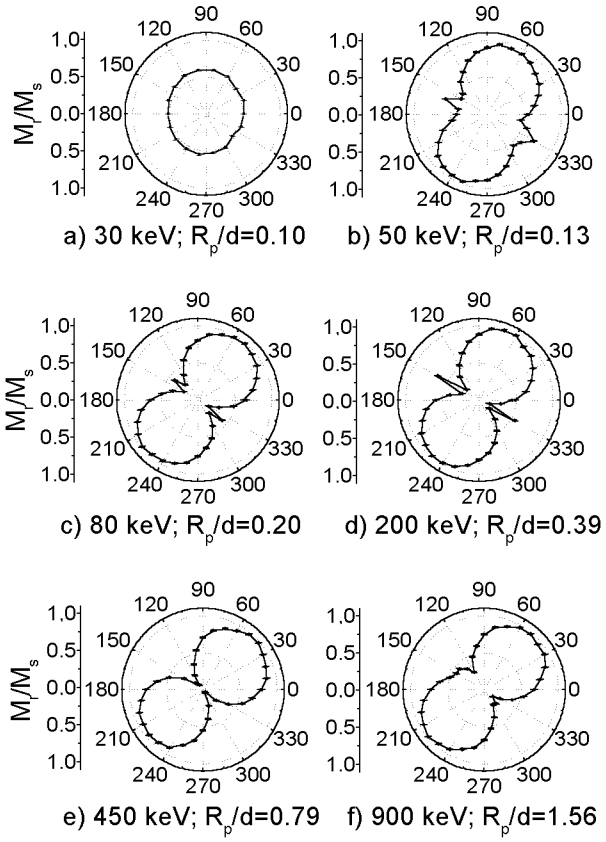

Fig. 6. MOKE patterns of the samples irradiated at different Xe-ion energies.

via Rutherford backscattering (RBS) (to check the Xe-profile), X-ray diffraction (XRD) (changes of lattice constant and local stresses), and MOKE (magnetic anisotropy). The lattice constant as obtained from XRD is shown in Fig. 5a, together with the FWHM of the (111) reflex (Fig. 5b) and the fraction f^{Ni} of Xe-ions stored in the Ni-film (Fig. 5c). Clearly, the mean lattice dilatation is largest when the ions are fully stored near the middle of the Ni layer ($\Delta a = 0.008$ Å). The lattice dilatation is reduced when either a large fraction passes the Ni foil and is stored in the SiO_2 substrate, or when Xe is deposited close to the surface, i.e. at a distance much smaller than the typical XRD scanning length. The evolution of magnetic remanence in this set of samples measured via MOKE is displayed in Fig. 6. One notes that magnetic anisotropy appears around $R_{\mathrm{p}}/d = 0.15$ and stays rather constant up to $R_{\mathrm{p}}/d \approx 0.8$, but then gets weaker ($R_{\mathrm{p}}/d = 1.56$, Fig. 6f).

In the second series of experiments, the effect of external stresses was studied in the following way: the 75 nm thick Ni films, 7×10 mm^2 in size, were deposited onto rectangular $\langle 100 \rangle$ Si substrates, 40×15 mm in size, which were then bent rel-

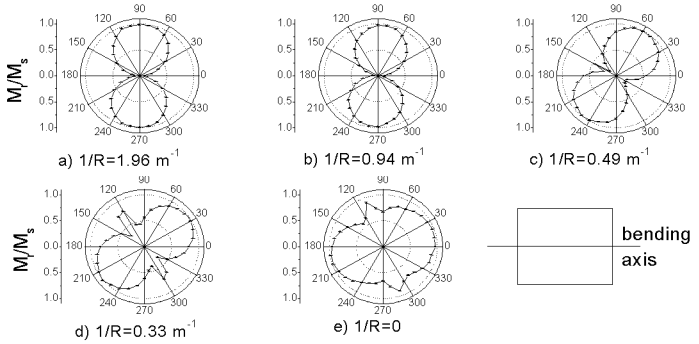

Fig. 7. MOKE pattern of the remanence in a 75 nm Ni layer on SiO_2 measured as function of the bending curvature $1/R$ of the samples during the 450 keV Xe implantations at 100 K.

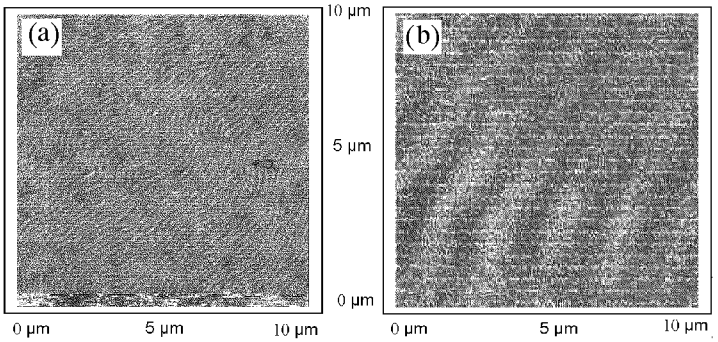

Fig. 8. MFM analysis of a 75 nm Ni film on Si: (a) as deposited, (b) irradiated with 4×10^{14} Xe/cm^2. Note the domains whose width has increased from 200 nm to 2 μm.

ative to one of the two axes. The curvature of each Ni film was measured by means of a profilometer and adjusted to a curvature of $0 \leq 1/R \leq 2$ m^{-1} (see Fig. 7). After the irradiations of the bent samples at 100 K with 4×10^{14} Xe-ions/cm^2 at 200 keV, the stress was released so as to provide a flat surface at room temperature, again checked with the profilometer, and MOKE analyses were carried out. The results are shown in Fig. 7. One notes that (1) the magnetic texturing effect, visible as the ratio of largest and smallest remanence, increases for increasing curvature $1/R$, and that (2) the pattern turns towards the axis perpendicular to the bending axis, for increasing curvature $1/R$. This is to be expected, since the release of the external stresses after implantation creates a compressive stress in the Ni film and leads to the magnetostrictive anisotropy parallel to this stress.

As a last result, the domain structure as measured via magnetic force microscopy (MFM) is shown in Fig. 8. The 75 nm Ni film had been deposited onto Si and irradiated with 4×10^{14} Xe-ions/cm^2 of 200 keV. One notes that the typical periodicity length of the domains increased from about 200 nm to 2 μm, as a consequence of the ion bombardment. This finding still needs to be explained.

4. Xe-irradiations of Fe films: magnetic anisotropy and microstructure

Similar investigations as described above for thin Ni films have also been carried out in the case of Xe-irradiated Fe films deposited onto Si and SiO_2 substrates. In this system, it is advantageous to use conversion electron Mössbauer spectroscopy (CEMS), which monitors the magnitude and orientation of the local hyperfine field. As can be seen in Fig. 9, the CEMS spectra of a 152 nm Fe film taken before and after a Xe-irradiation at 450 keV and 100 K show a distinct change of the intensities of the hyperfine components of the sextet. This change of the intensity ratio indicates that the magnetization of the film, which originally was almost isotropic, has switched into the film plane, due to the Xe-implantation. Preliminary CEMS studies with the sample inclined relative to the direction of the photon beam proved that one can also determine the axis of preferred magnetization in the foil via CEMS.

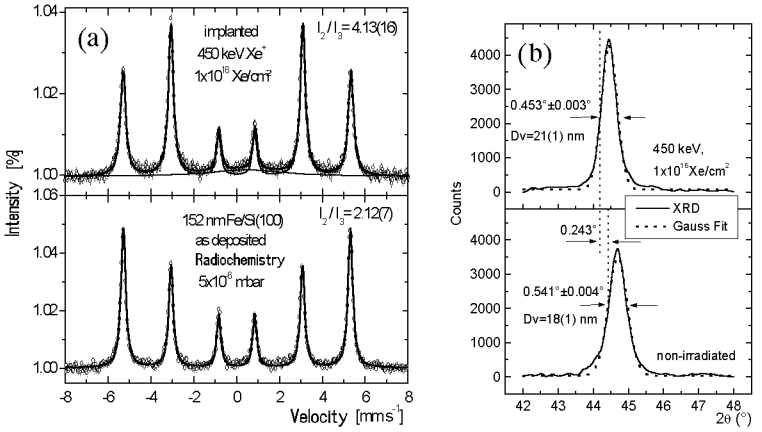

Fig. 9. (a) CEMS spectra of a 152 nm Fe film, irradiated with 1×10^{16} Xe-ions/cm^2 at 450 keV and 100 K. (b) XRD spectra of the 152 nm Fe film, before and after irradiation with 1×10^{16} Xe-ions/cm^2 at 450 keV and 100 K.

As to the XRD spectra of this sample displayed in Fig. 9b, we observe a shift of the position of the $\langle 100 \rangle$ reflex by $2\Delta\theta = 0.243°$, corresponding to a change in the lattice constant by 0.4%, but no significant ion-induced increase in the grain size ($D_V = 18(1)$ nm before irradiation, $D_V = 21(1)$ nm after irradiation). Hence no ion-induced grain growth appears to happen as found for similar irradiations of Ag layers [19, 20].

5. Summary

In continuation of our previous work on ion irradiated ferromagnetic films [8, 9, 13, 15], we have shown that Xe-irradiations of thin polycrystalline Ni and Fe

films produce strong magnetic polarization effects, visible as pronounced anisotropies of the magnetic remanence M, saturation field H_a and coercive field H_c. In the process one may distinguish two stages: upon low-fluence Xe-implantation, the magnetic field switches from a more or less isotropic spatial distribution into the film plane, as demonstrated by PAC and CEMS (in the case of Fe), and the coercive field H_c is strongly reduced (as demonstrated by MOKE). A second effect is the in-plane polarization of the magnetization along certain axes, called magnetic texturing here. We have studied the influence of various parameters, as for example the ion range (relative to the film thickness) and the external stresses during implantation. The dependence of the magnetic anisotropy of an external polarizing magnetic field, on the implantation and annealing temperature and on multiple irradiations will be discussed separately. First analyses via MFM and VSM have been carried out, but more detailed experiments are needed.

Inverse magnetostriction [21, 22] and an external magnetic field during implantation are among the decisive parameters governing the magnetic texturing effect. As the local stresses depend in a complicated way on the conditions of the film deposition process, the range and density of the implanted (insoluble) noble gas ions and wanted or unwanted external stresses, no full separation into these components has been possible so far. The XRD spectra reveal lattice dilations due to the implanted Xe-ions, but rather little ion-induced grain growth.

Acknowledgments

We are grateful to Sönke Habenicht and Detlev Purschke for their help with the ion implantations at IONAS and IOSCHKA [23, 24]. We also acknowledge the assistance of Norbert Quaas, Konrad Samwer, and Martin Wenderoth (Göttingen) with the MFM and VSM analyses and helpful discussions with Harry Bernas (Orsay), Martin Farle (Braunschweig), Ulrich Gradmann (Clausthal), Jürgen Hesse (Braunschweig), and Martin Sander (Halle).

References

[1] J. Kanamori, in: *Magnetism*, Vol. 1, Eds. G.T. Rado, H. Suhl, Academic Press, New York 1963, p. 127.

[2] A. Hubert, R. Schäfer, *Magnetic Domains*, Springer-Verlag, Berlin 2000; K.J. Kirk, *Contemp. Phys.* **41,** 61 (2000).

[3] C. Chappert, H. Bernas, J. Ferré, V. Kottler, J.P. Jamet, Y. Chen, E. Gambril, T. Devolder, F. Rousseaux, V. Mathet, H. Launois, *Science* **280,** 1919 (1998).

[4] T. Aign, P. Meyer, S. Lemerle, J.P. Janet, J. Ferré, V. Mathet, C. Chappert, J. Gierak, C. Vieu, F. Rousseaux, H. Launois, H. Bernas, *Phys. Rev. Lett.* **81,** 5656 (1998).

[5] J. Ferré, C. Chappert, H. Bernas, J.P. Jamet, P. Meyer, O. Kaitasov, S. Lemerle, V. Mathet, F. Rousseaux, H. Launois, *J. Magn. Magn. Mater.* **198/199,** 191 (1999).

[6] B.D. Terris, D. Weller, L. Folks, J.E.E. Baglin, A.J. Kellock, H. Routhuizen, P. Vettiger, *J. Appl. Phys.* **87,** 7004 (2000).

[7] W.A. Lewis, M. Farle, B.M. Clemens, R.L. White, *J. Appl. Phys.* **75,** 564 (1994).

[8] M. Neubauer, P. Schaaf, M. Uhrmacher, K.P. Lieb, *Phys. Rev. B* **53,** 102 (1996).

[9] N. Reineke, diploma thesis, Göttingen 1997, unpublished.

[10] M. Neubauer, P. Wodniecki, M. Störmer, W. Bolse, H.U. Krebs, M. Uhrmacher, K.P. Lieb, in: *XXXII Zakopane School of Physics*, Eds. E.A. Görlich, K. Latka, Wyd. Uniwersytetu Jagiellońskiego, Kraków 1997, p. 56.

[11] D. Kurowski, R. Meckenstock, J. Pelzl, K. Brand, P. Sonntag, P. Grünberg, *J. Appl. Phys.* **81,** 5243 (1997); *Mater. Sci. Forum* **248/249,** 177 (1997).

[12] M. Neubauer, K.P. Lieb, M. Uhrmacher, P. Wodniecki, *Europhys. Lett.* **43,** 177 (1998); *Hyperfine Interact.* **120/121,** 331 (1999).

[13] M. Neubauer, M. Reinecke, M. Uhrmacher, K.P. Lieb, M. Münzenberg, W. Felsch, *Nucl. Instrum. Methods Phys Res. B* **139,** 332 (1998).

[14] E. Gu, J.A.C. Bland, C. Daboo, M. Gester, L.M. Brown, R. Ploessl, J.N. Chapman, *Phys. Rev. B* **51,** 3596 (1995); J.M. Florczak, E.D. Dahlberg, *Phys. Rev. B* **44,** 9338 (1991); *J. Magn. Magn. Mater.* **104,** 399 (1992).

[15] Kun Zhang, K.P. Lieb, P. Schaaf, M. Uhrmacher, W. Felsch, M. Münzenberg, *Nucl. Instrum. Methods Phys. Res. B* **161-163,** 1016 (2000).

[16] K.N. Tu, W.K. Chu, J.W. Mayer, *Thin Solid Films* **25,** 403 (1975); D.M. Scott, M.-A. Nicolet, *Nucl. Instrum. Methods* **182/183,** 655 (1981); M. Milosavljevic, S. Dhar, P. Schaaf, N. Bibic, K.P. Lieb, *Appl. Phys. A* **43,** 71 (2000); *J. Appl. Phys.* **90,** 4478 (2001).

[17] J.P. Biersack, program TRIM95, private communication.

[18] P. Wodniecki, T. Corts, K.P. Lieb, M. Uhrmacher, *Nucl. Instrum. Methods Phys. Res. B* **62,** 394 (1992).

[19] A. Crespo-Sosa, P. Schaaf, W. Bolse, K.P. Lieb, *Phys. Rev. B* **53,** 14795 (1996); in: *Proc. "CAARI-96", Denton (USA) 1996*, American Institute of Physics, 1997, p. 945.

[20] K.P. Lieb, *Contemp. Phys.* **40,** 385 (1999).

[21] D. Sander, *Rep. Prog. Phys.* **62,** 809 (1999).

[22] D. Sander, A. Enders, J. Kirschner, *J. Magn. Magn. Mater.* **200,** 439 (1999).

[23] M. Uhrmacher, K. Pampus, F.J. Bergmeister, D. Purschke, K.P. Lieb, *Nucl. Instrum. Methods Phys. Res. B* **9,** 234 (1985).

[24] S. Habenicht, W. Bolse, K.P. Lieb, *Rev. Sci. Instrum.* **69,** 2120 (1998).